

## 2-2 Electromagnetic prospecting TEM method

### 2-2-1 Object of survey

The object of the electromagnetic prospecting TEM method is to make clear details of its resistivity structure around the IP anomaly zone extracted by the IP prospecting survey, and to extract potential zones for ore deposits. The IP anomaly zone and magnetic anomaly zone are characteristically overlapped in the survey area, therefore special emphasis is put on clarification of its extension to the depth.

### 2-2-2 Location and contents of the Survey

The TEM method has been applied for the Azzouz and Khefawna districts out of six districts where the IP method was previously conducted. Reason why the Azzouz district was chosen for the TEM survey, is that the north to south trending high IP anomaly was detected, and the magnetic anomaly was overlapped in the district. Figure II-2-2-2 shows the location of the survey points. In the TEM survey, inversion of the polarization has happened, at some points, so the additional different configuration of the transmitter and receiver has been also applied.

In the Khefawna district, The TEM method has been performed for the detected high magnetic anomaly zone.

Table II-2-2-1 shows the contents of the survey

Table II-2-2-1 Number of TEM survey stations

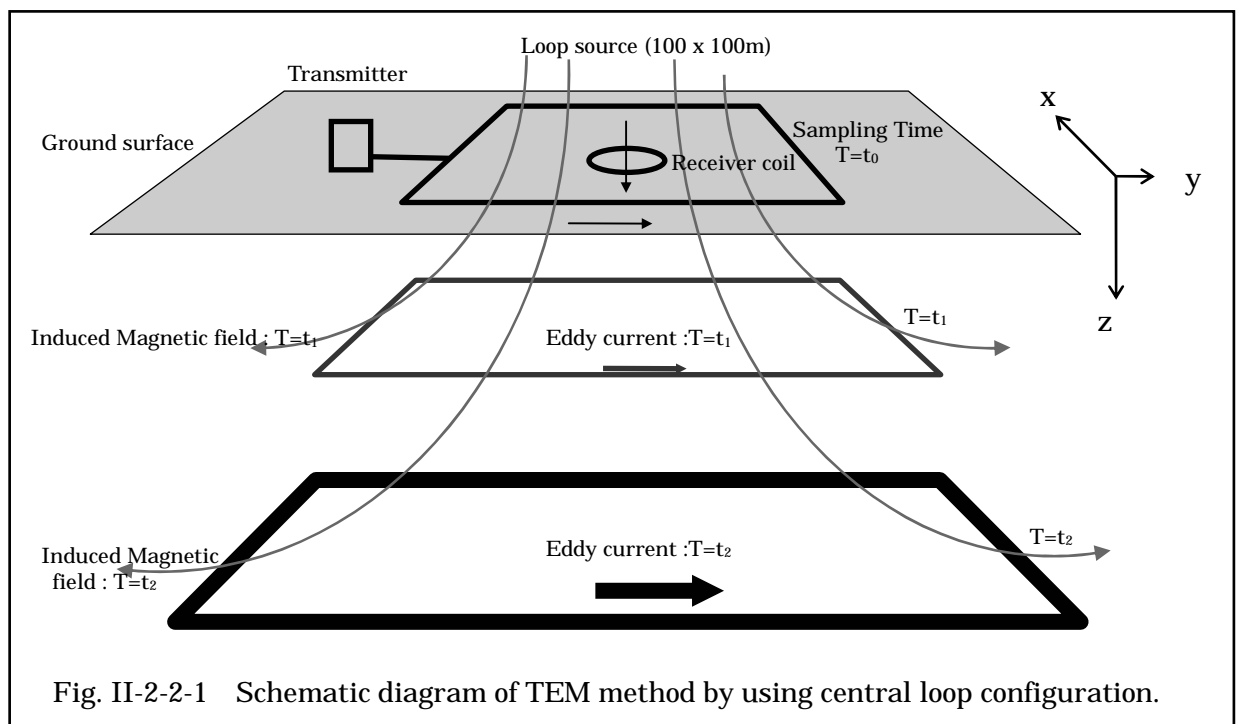
Area name	Tx-Rx configuration	Number of stations	Length of survey lines
Azzouz	In loop	146	
	Fixed loop		300m*3lines*2loop
Khefawna	In loop	19	
Total		165	1,800m

### 2-2-3 Survey method

For the measurement instrument, the product of Canadian Geonics has been used in the survey. The data recorder "PROTEM(D)" equips multiple measuring range within the sampling time 0.00613 ms to 69.78 ms to obtain the magnetic field deviation rate after transmitting shut down. In the last year's survey, the central loop configuration with 100 m x 100 m transmitting loop was adopted, and the measurement range was 0.00613 ms to 0.06959 ms in u-mode, 0.08813 ms to 6.978 ms

in H-mode, and 0.8813 ms to 69.78 ms in L-mode. However, in some districts, the resistivity structure could not analyzed in the target depth of 200 m due to the IP affection or weak signal. Therefore, the large scale 500 m × 500 m in-loop configuration has been applied to increase output signal intensity. EM37 has been used for the transmitter, and the transmitting current has been around 18 ampere. Due to the large scale loop, the crystal-mode have been applied to synchronize both clocks installed in the transmitter and receiver, and the measurement range has set to H-mode. The delay time (turn off time), which indicates the time from transmitting shut off to sampling start, was set to 0 microsecond .and 1,000 microsecond (in two modes) for the measurement to obtain the deeper information.

Figure II-2-2-1 shows schematic diagram of TEM method by using central loop configuration.



The data inverted its polarity of measured potential has been obtained at two points in the Azzouz district in this survey. Usually, the polarity is in the same direction in the in-loop configuration, therefore the inversion might be happened due to some environment existing some magnetic material underneath. These magnetic material would be some ores, graphite, argillization zone, fault etc. or some sulfide minerals as some source caused IP anomaly. It is possible that inversion phenomena is

caused by existence of some ores, therefore search its shape of unknown material is necessary. The fixed loop configuration has been adopted to achieve this object.

#### 2-2-4 Analytical method

The measured potential  $V_0$ (mV) from PROTEM(D) can be converted to the magnetic field deviation rate  $dB/dt$ (nV/m<sup>2</sup>) by the following formula.

$$\frac{dB}{dt} = \frac{V_0 \cdot 19200}{E \cdot 2^n} \quad (2-2-1)$$

Whereas  $E$ (m<sup>2</sup>) is effective area of receive coil; and  $2^n$  is amplified gain. Furthermore, the magnetic field deviation can present by the apparent resistivity

$\rho_a(t)$  (· m) of the time function by the following formula.

$$\rho_a(t) \cong \frac{\mu}{4 \pi t_c} \left( \frac{2 \mu M}{5 t_c dB/dt} \right)^{2/3} \quad (2-2-2)$$

Whereas  $\mu$  is magnetic permeability ( $4 \times 10^{-7}$  H/m), and  $t_c$ (msec) is delay time after transmitting shut off,  $M$  is moment of transmitter, product of area of transmitter loop (m<sup>2</sup>) and current of transmitting (A).

The one dimensional multilayer structural analysis has been performed using the apparent resistivity values obtained by the formula 2-2-2. TEMIXXL of INTERPEX Co. has been used for the analysis. In this one dimensional analysis, the bind-conditioned multi layer structure analysis called "Occams inversion" has been adopted. The one dimensional multi layer analysis has been performed based on this "Occams inversion" result as the initial model.

For the data obtained from the fixed loop configuration measurement, the plate model analysis has been applied for each survey line. In the analysis, the magnetic field deviation rate for each different plate size, position, and conductivity is obtained putting some conductive plate into homogeneous media, and try to obtain its coincident value of theoretical value and measured value. The software MOTEM of GEONIC Co. has been used for the analysis.

## 2-2-5 Survey result

### 2-2-5-1 Measurement result

In the measurement this time, the two mode measurement, delay time=0  $\mu$  sec and 1,000  $\mu$  sec, in H mode has been performed. The analysis software TEMIXXL can not input two data in the same measuring range simultaneously. So that the front half data in the 0  $\mu$  sec mode and the rear half data in the 1,000  $\mu$  sec mode are merged using some text editor, to treat as one data. The overlapped part of these two modes is neglected by this process, the final sampling number becomes 30, called gate 1, 2, 3, ----- 30 from the faster time order. The measured data for each measuring point are shown in the appendix as the “Magnetic field deviation rate versus Time curves” and “Apparent resistivity versus Time curve”.

### Azzouz district

#### 1) Measurement result of in-loop configuration

The measurement result in the district is relatively good. In the northern district, some noise probably caused by power lines along roads have been noted, but no harm for the analysis. Figure II-2-2-3 shows the distribution of the magnetic field deviation rate. In the figure, the rate of gate 1 to gate 30 are arranged from left-upper to right lower, and indicates a general trend of transition from high to low magnetic field deviation. The data at the survey point 900N500E in the central part shows negative from gate 4, and it continues to the gate 30. At the survey point 030N050E, the values from gate 20 to gate 25 show negative. At the gate 1 to gate 6, reflecting the surface, some high magnetic field deviation anomaly is recognized in the central western part, indicating existence of some high resistivity zone.

Figure II-2-2-4 shows the measuring points indicating negative values in the magnetic field deviation rate and the “magnetic field rate versus time” curve around those points. Around the points showing magnetic field polarization inversion, it is recognized that the data of inverted gates distorts toward down side. It is presumed that the distortion is occurred by the same cause as that in the inversion due to its continuity. Pseud-high resistivity layers are analyzed at the distortion parts in the one dimensional multi-layer structural analysis for these data, therefore these resistivity structure is not shown in the figure of plane and cross section.

#### 2) Measurement result in fixed loop configuration

The polarization inversion is recognized at the measuring point 090N050E in the in-loop configuration measurement, and similar indication is seen around the point. The fixed loop configuration measurement is performed to clarify its cause. The transmitter and receiver configuration is very sensitive for conductive plates, therefore it is thought that the measurement by this configuration can produce good result to reveal its figure of plate, if it exists.

The transmitter loop is set to the southeast of the target point, and its size is 100 × 200 m. Three survey lines extending in the northwest from the center of the transmitter loop, and the point spacing is 25 m. The measurement has been performed in the H-mode and the delay time set at only 0 μ sec.

Figure II-2-2-8 shows the profile of the magnetic field deviation for each survey line. The profile shows from the gate 1 to 10, and the magnetic field deviation of the gate 10 is shown on the back. The polarity inversion is seen in the early stage in the survey lines 950N, 900N, and 850N, and the line connecting the inversion points directs toward north 10 degrees east. In the survey lines 400N, 350N, and 300N, all gates show polarity inversion, and the line connecting those points directs towards north 31 degrees east.

Usually, the magnetic field obtained outside of transmitting loop inverts its polarity earlier from the early time stage magnetic field accordingly their distance from the loop. In case of measuring in homogeneous media, profiles moving their inversion time are drawn. Accordingly, the result of the measurement in this survey indicates existence of underground heterogeneous resistivity structures.

#### Khefawna district

The measurement data in the district is very good due to no noise source around the area. Figure II-2-2-11 shows the profiles arranged survey points east to west. The profile shows the gate from 1 to 10, and the magnetic field deviation rate of the gate 1 is on the background. No abrupt deviation is seen in the profiles, but it tends to lower toward the southeast from the center.

#### 2-2-5-2 Analytical result

##### 1) Result of Occams inversion analysis by in-loop configuration

Figures II-2-2-5 and II-2-2-6 show the planes and cross sections of the result of the Occams inversion analysis. The resistivity structure of each cross section shows

generally three layers structure, medium resistivity layer around 150  $\Omega \cdot m$ , high resistivity layer higher than 500  $\Omega \cdot m$ , and medium resistivity layer lower than 150  $\Omega \cdot m$  from the surface. In the further deeper part, a low resistivity layer, lower than 500  $\Omega \cdot m$ , is analyzed in the northwest side. In the cross section 500N to 300N, a high resistivity zone around 500  $\Omega \cdot m$  is detected in an area about 300 m in altitude in the southeastern part. In the plane, a high resistivity zone higher than 300  $\Omega \cdot m$  is distributed near the surface, about 400 m in altitude, and some resistivity contrast changing east to west is recognized in the 300 m level. The low resistivity zone in the 300 m level seen in the cross section is not detected in the 100 m level. A part of the high resistivity zone, trending north to south and higher than 500  $\Omega \cdot m$ , continues to the 100 m level.

## 2) Result of one dimension multi layer structural analysis by in-loop configuration

In the analysis, the resistivity structure of the Occams inversion is given as the initial model, and it tries to obtain the most suitable resistivity structure for the Resolution Matrix and minimum RMS error. Figure II-2-2-7 shows the result of the analysis, however the obtained resistivity structure is present in a columnar section.

The outline of the resistivity structure tends to similar to the result of the Occams inversion analysis. In the cross section 1600N to 1100N, a three layer structure, around 150  $\Omega \cdot m$  and less than 100 m thick (First layer), around 1,000  $\Omega \cdot m$  and about 150 m thick (Second layer), and 100  $\Omega \cdot m$  (Third layer) from the surface, is analyzed. In the cross section 100N, a three layer structure is similarly analyzed, but the resistivity of the second layer is lower than 1,000  $\Omega \cdot m$ .

In the cross section 900N to 100N, the first layer is constant in 150  $\Omega \cdot m$  to 250  $\Omega \cdot m$  and about 50 m thick, but the lower part shows slightly complicated structure. A big change in the resistivity is recognized between the northwest side and southeast side bounded by the central zone, higher than 200  $\Omega \cdot m$  in the northwest side and around 100  $\Omega \cdot m$  in the southeast side. In the southeast side of the cross section 400N and 300N, a low resistivity zone, lower than 50  $\Omega \cdot m$ , is analyzed in the 300 m level. In the deeper part of the northwest side, a low resistivity layer, around 50  $\Omega \cdot m$ , is analyzed dipping to the southeast.

## 3) Result of plate model analysis

Figures II-2-2-9(1) and II-2-2-9(2) show the result of the plate model analysis

for each profile, and Table II-2-2-2 shows param of the model.

The model obtained by the analysis is a conductive plate, 300 × 200 m in size in the section 400N to 300N, N 10 E strike and 70 E dip. In the section 400N to 300N, a conductive plate 400 × 350 m in size strikes N 31 E and 45 to 70 E dip. Almost same parameter is effective for the plate detected in the all three survey lines between 950N and 850N, for the all gate. Contrary, the plate size and strike between 400N and 300N is not changed, but the position, dipping, and conductivity of the plate is variable, i.e. the conductivity is greater in the late gate (deeper part) and shows gentle dipping in the deep part in 400N.

#### Khefawna district

Figures II-2-2-12 and II-2-2-13 show the result of the Occams inversion analysis. The shallow part from the surface to the 500 m in altitude level shows low resistivity below 50 Ω·m, and further lower part shows high resistivity zone above several hundreds Ω·m is analyzed. The high resistivity layer is nearly flat in the northern cross section 2300N, on the contrary it shows slightly convex shape in the central cross sections 2200N and 2300N. This structure is also pointed out from the resistivity structure plane, the low resistivity layer is distributed centering the central part near the surface level 600 m in altitude, and the high resistivity layer higher than several hundreds Ω·m around 400 m level shows dome-like shape, extending to the southeast.

#### 2-2-6 Consideration

The TEM method has been applied in this year's survey to make clear the extension of the IP anomaly zones detected by the previous survey. The target areas are the Azzouz and Khefawna districts. The measurement has been performed using the large transmitting loop, 500 x 500 m, with the in-loop configuration. The fixed loop configuration measurement also has been applied in some part of the Azzouz district. Followings are the characteristics of each district.

##### (1) Azzouz district

In the district, the magnetic field inversion has been observed in the central and southern parts, simultaneously some data indicating some affection of the IP effect has been observed. Based on the result of the one dimensional analysis, it has revealed

that the resistivity structure in the district is different in the northern side and southern side of the survey line 1000N. The three continuous layer structure, the medium resistivity layer (around 150  $\cdot$  m), high resistivity layer (1,000  $\cdot$  m), and slightly low resistivity layer (100  $\cdot$  m) from the surface, exists in the northern side. The horizontally discontinuous structure, 200  $\cdot$  m in the northwestern side and 100  $\cdot$  m in the southeastern side, is recognized below 400 m depth. In the southeastern side of the cross sections 400N and 300N, the low resistivity zone below 50  $\cdot$  m has been analyzed around the level 300 m in altitude. The conductive plate has been analyzed at the point, where the polarity inversion was observed.

Figure II-2-2-10 shows the resistivity structure model of the Azzouz district, based on the above mentioned result. The figure shows the area affected the IP effect and analyzed conductive plate, in addition to the resistivity structure.

The TEM survey district is broadly underlain by the Paleozoic on the surface, and the geological structure is rather complicated due to various scale fault system. The analyzed resistivity structure reflect the geological structure, more complicated to the south. In addition to the complicated resistivity structure, some anomaly zone presumably related with potential ores have been detected at following points.

- (1) Central part, around measuring point 090N050E
- (2) Southern part, around measuring points 040N055 and 030N060E

In the point (1), the conductive plate is presumably surrounded by the IP anomaly zone, and its depth is shallower than 200 m. The conductivity is not so high, 1.5 S. On the other hand, in the point (2), the conductive plate extends to the depth of 350 m, and the IP anomaly zone is presumably situated in the northern side. Furthermore, the conductivity is higher to deeper, maximum value higher than 30 S. It is judged, therefore, that the first priority for the prospecting should be given to the point (2).

## (2) Khefawna district

The gentle dome-like high resistivity layer higher than several hundreds  $\cdot$  m has been detected by the TEM survey, and its extension to the southeast has been confirmed. The low resistivity layer lower than 50  $\cdot$  m broadly overlies the high resistivity layer. The high resistivity layer is presumably correlated to the syncline folding structure trending east to west, however further investigation is needed to verify the hypothesis.





LEGEND



Tx loop and measuring station  
by In loop configuration



Tx loop and measuring station  
by Fixed loop configuration

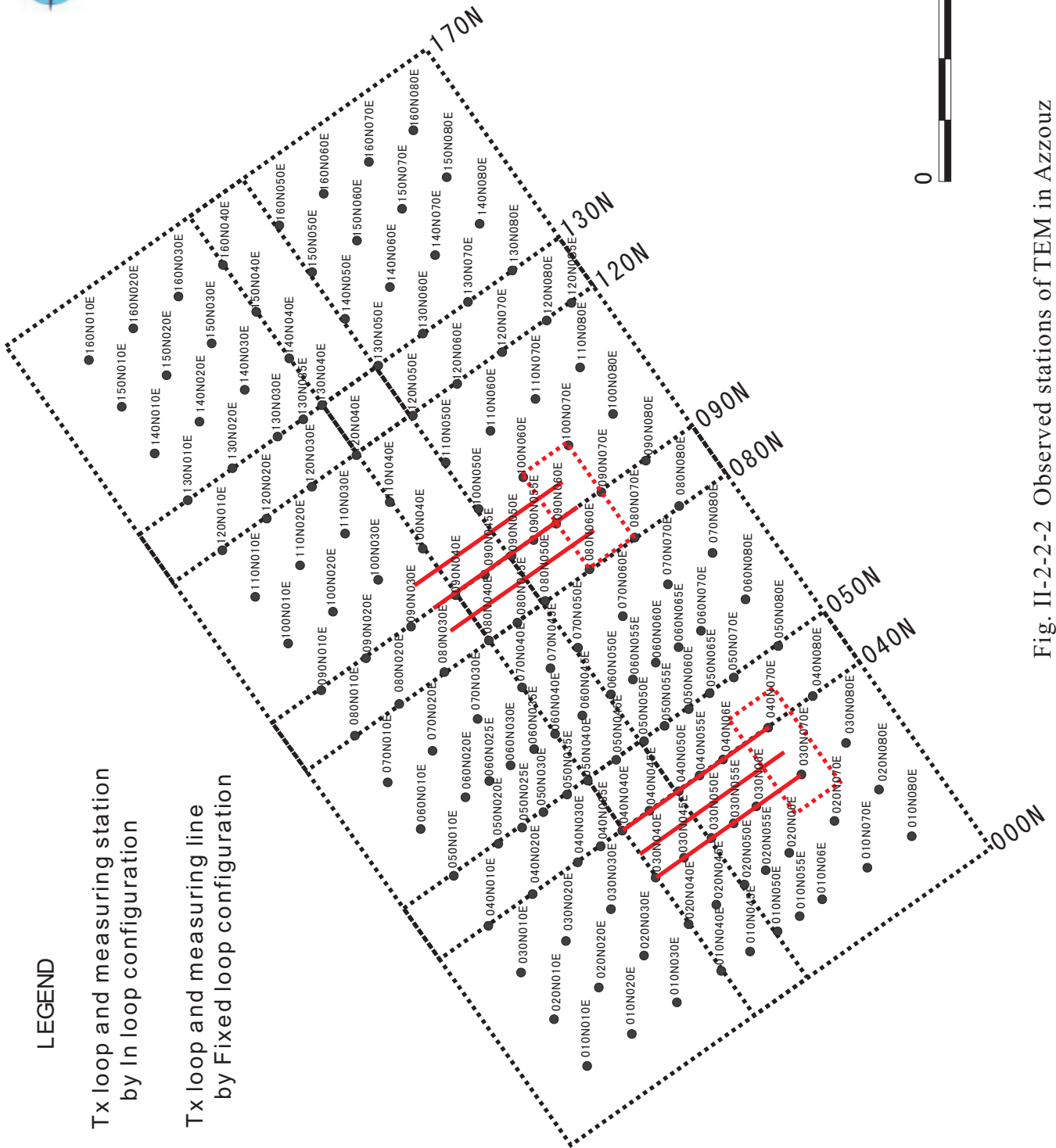


Fig. II-2-2-2 Observed stations of TEM in Azzouz

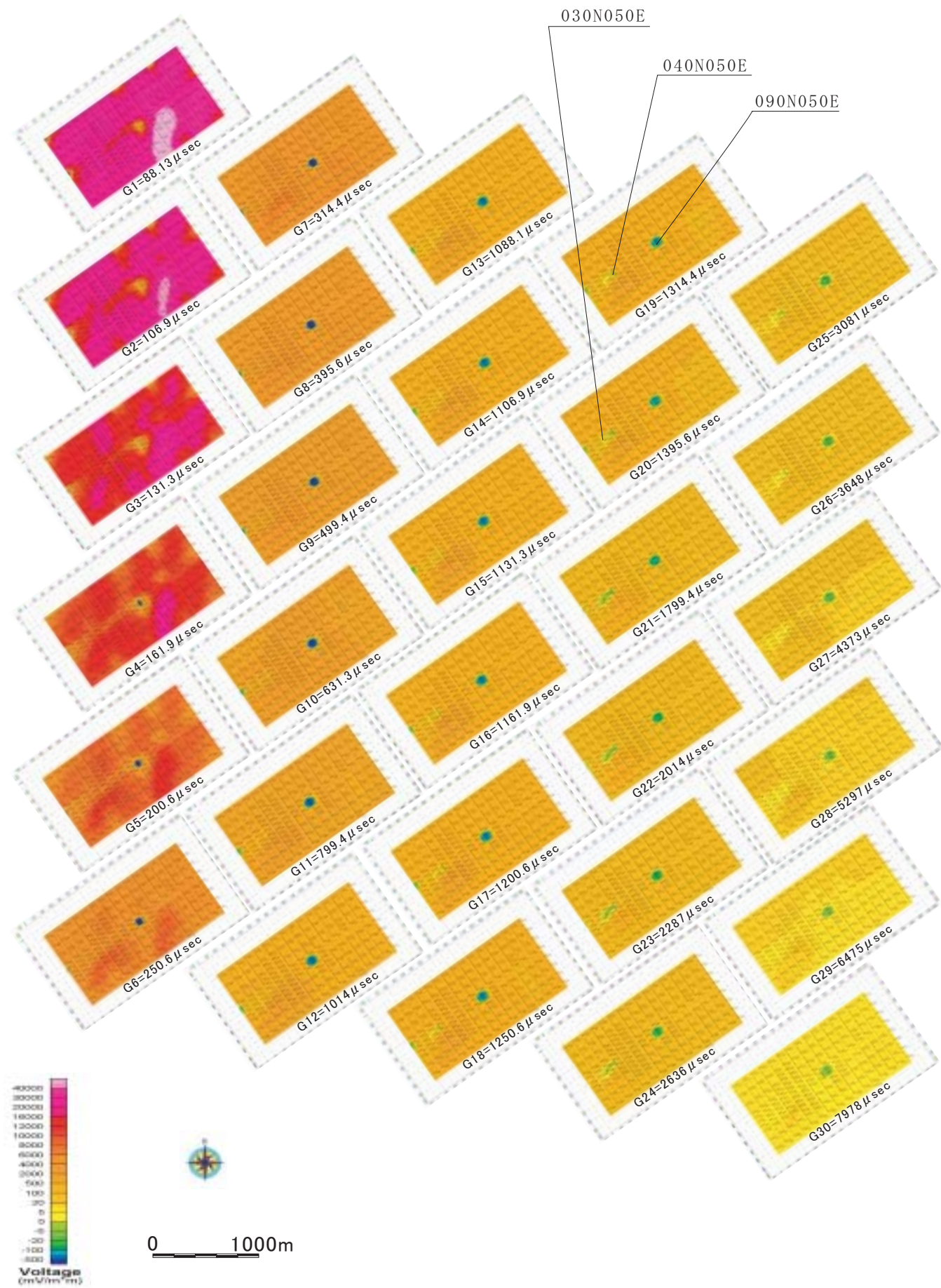


Fig. II-2-2-3 Normalized Voltage distribution map in Azzouz

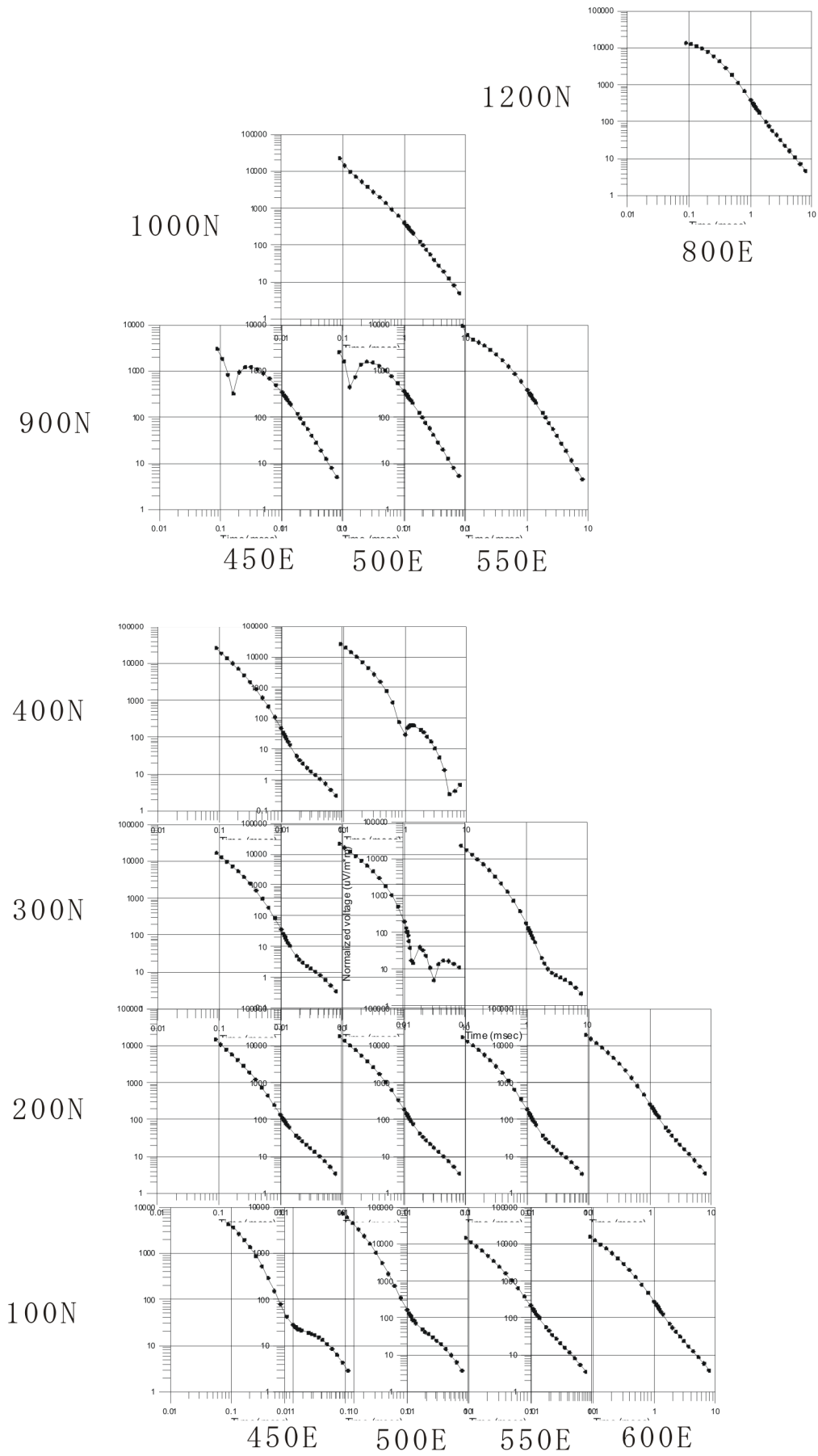


Fig. II-2-2-4 Transient Curve which are influenced by IP in Azzouz

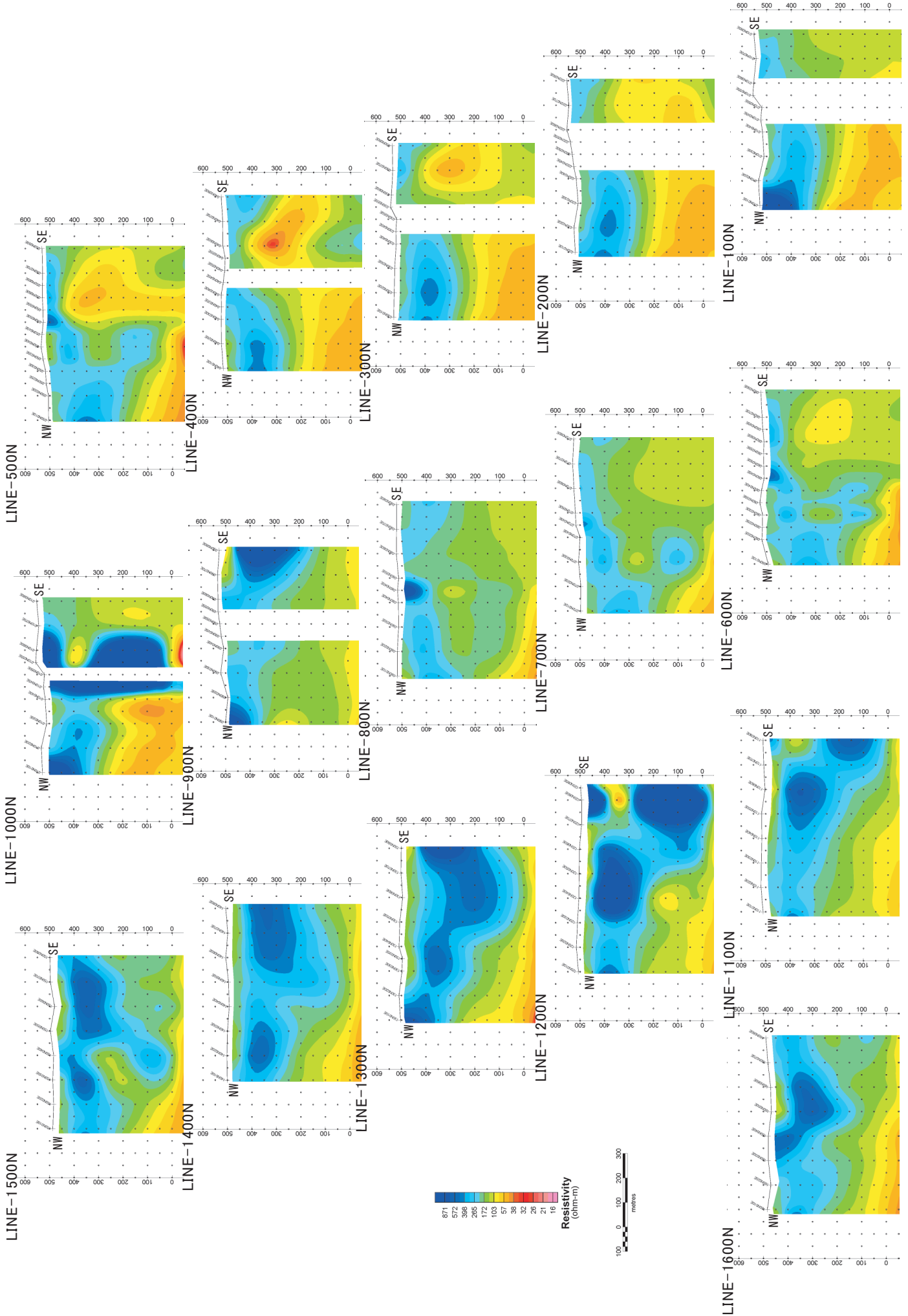


Fig. II-2-2-5 Resistivity structure sections by Occams inversion in Azzouz

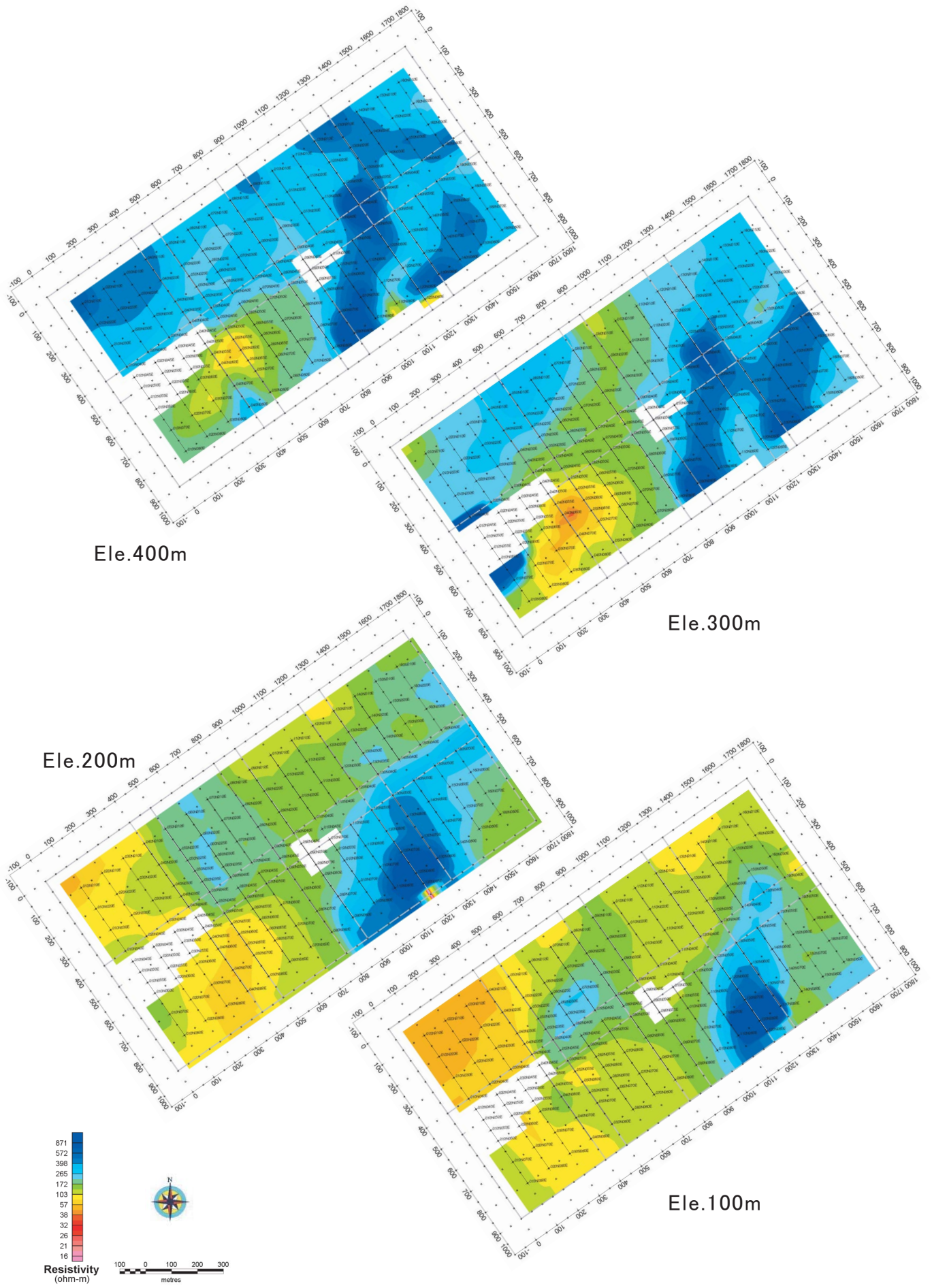


Fig. II-2-2-6 Resistivity distribution maps by Occams inversion in Azzouz

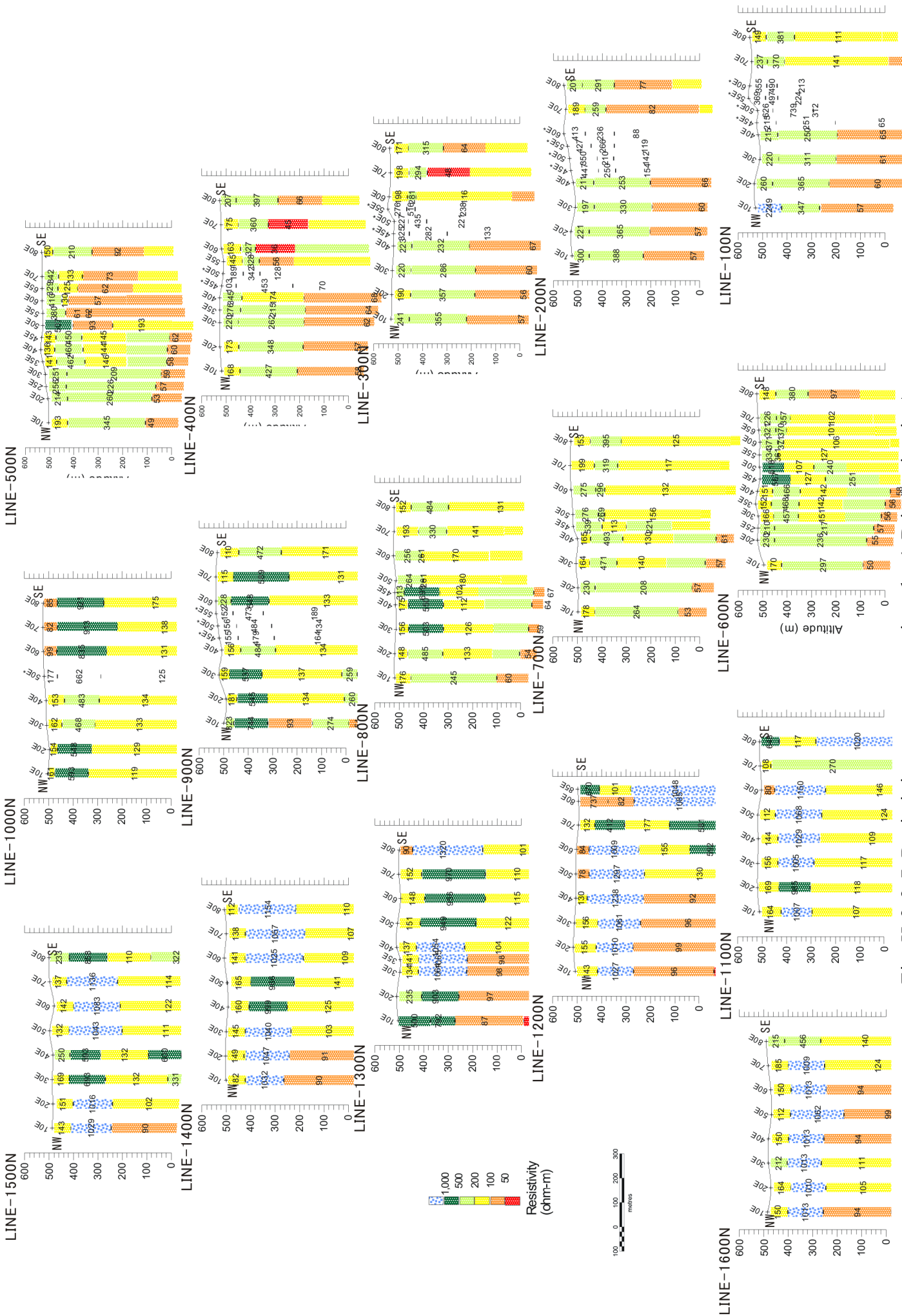


Fig. II-2-2-7 Resistivity structure sections by 1-D inversion in Azzouz

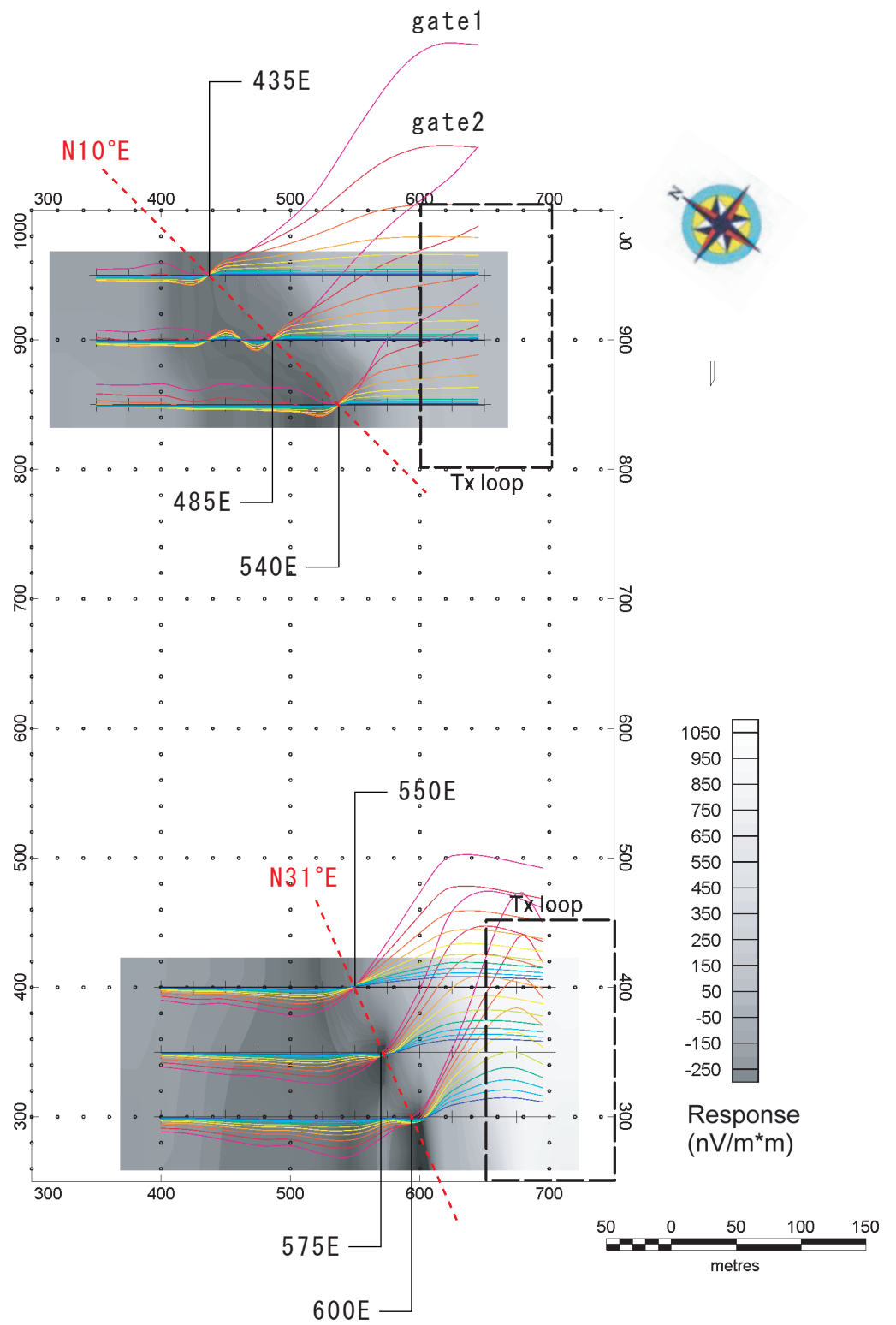


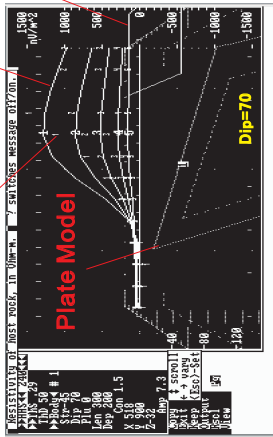
Fig. II-2-2-8 Normalized voltage profile by fixed loop configuration in Azzouz

Calculated Response

Observed response

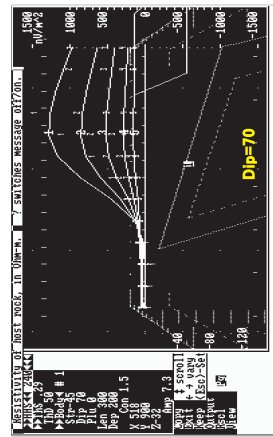
Tx loop

Line\_950N



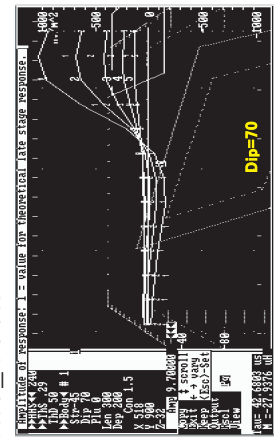
Gate1-5

Line\_900N

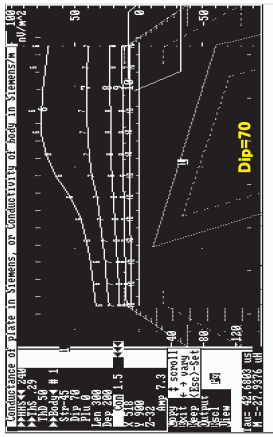


Gate1-5

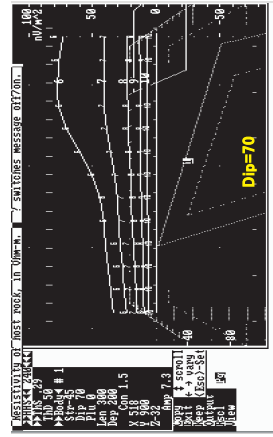
Line\_850N



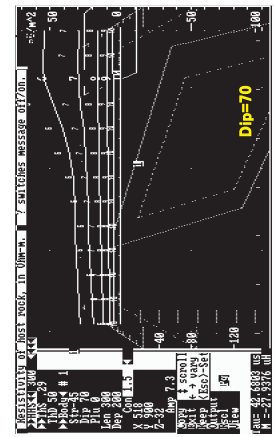
Gate1-5



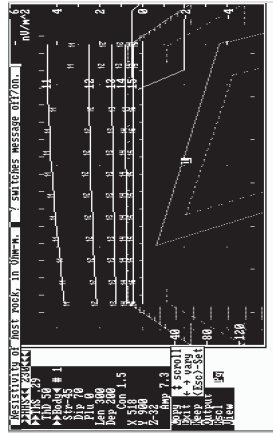
Gate6-10



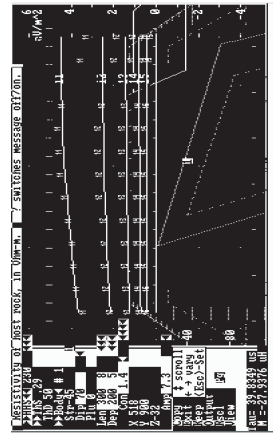
Gate6-10



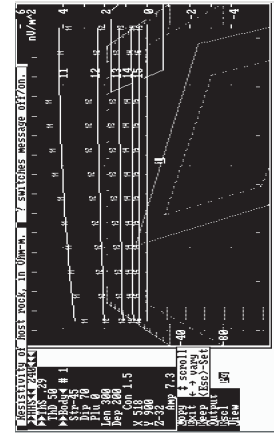
Gate6-10



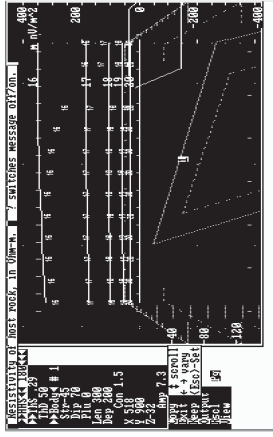
Gate11-15



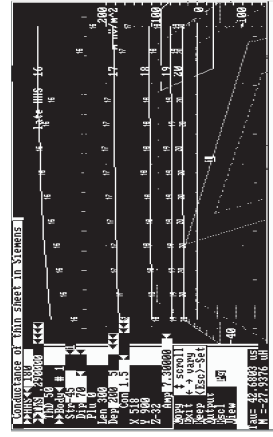
Gate11-15



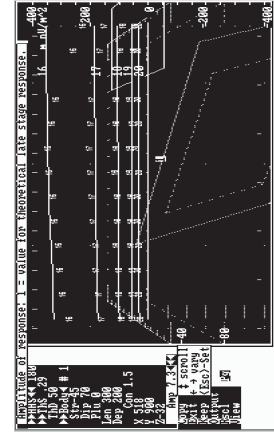
Gate11-15



Gate16-20



Gate16-20



Gate16-20

Fig. II 2-2-9(1) The result of simple plate analysis (1)

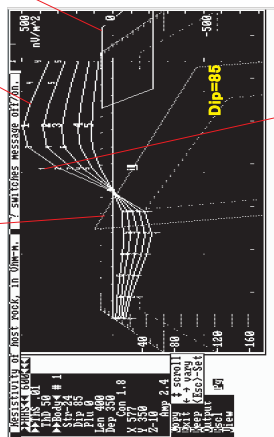


Calculated Response

Plate Model

Tx loop

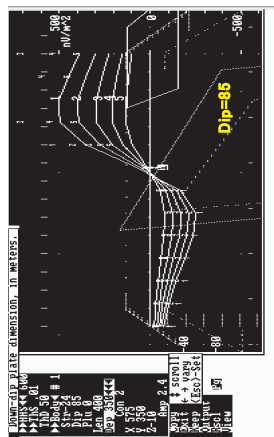
Line\_400N



Gate1-5

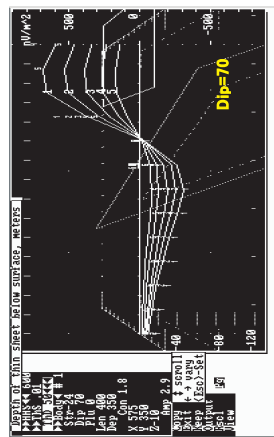
Observed response

Line\_350N

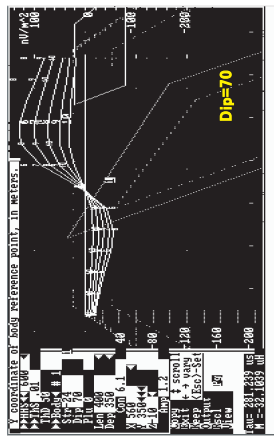


Gate1-5

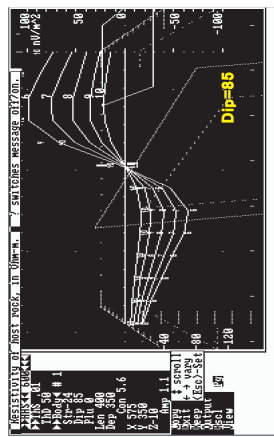
Line\_300N



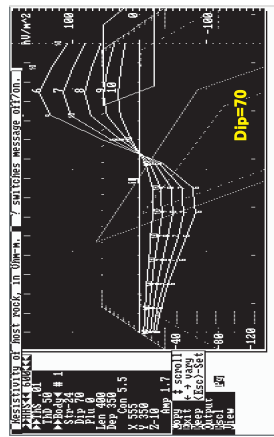
Gate1-5



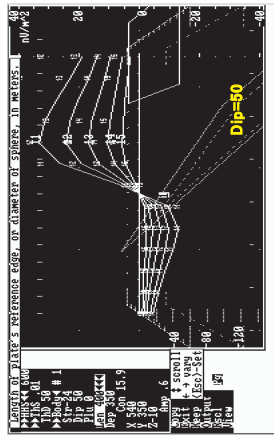
Gate6-10



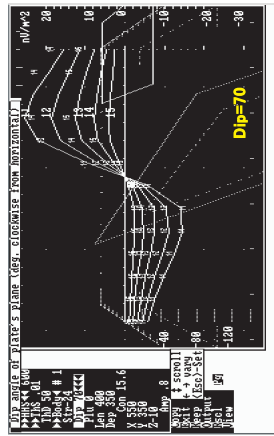
Gate6-10



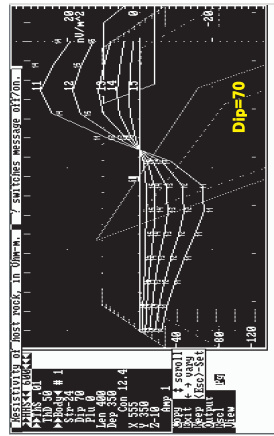
Gate6-10



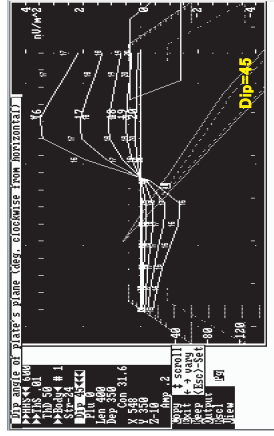
Gate11-15



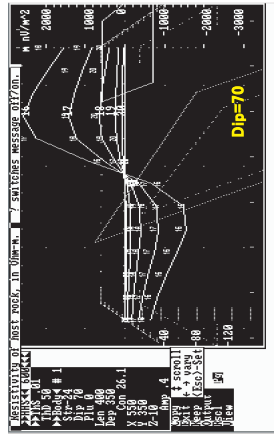
Gate11-15



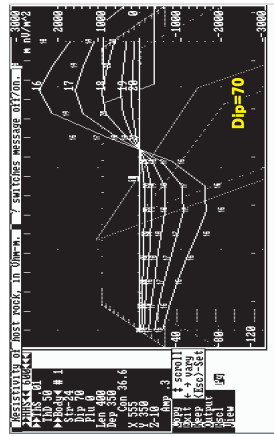
Gate11-15



Gate16-20



Gate16-20



Gate16-20

Fig. II 2-2-9(2) The result of simple plate analysis (2)

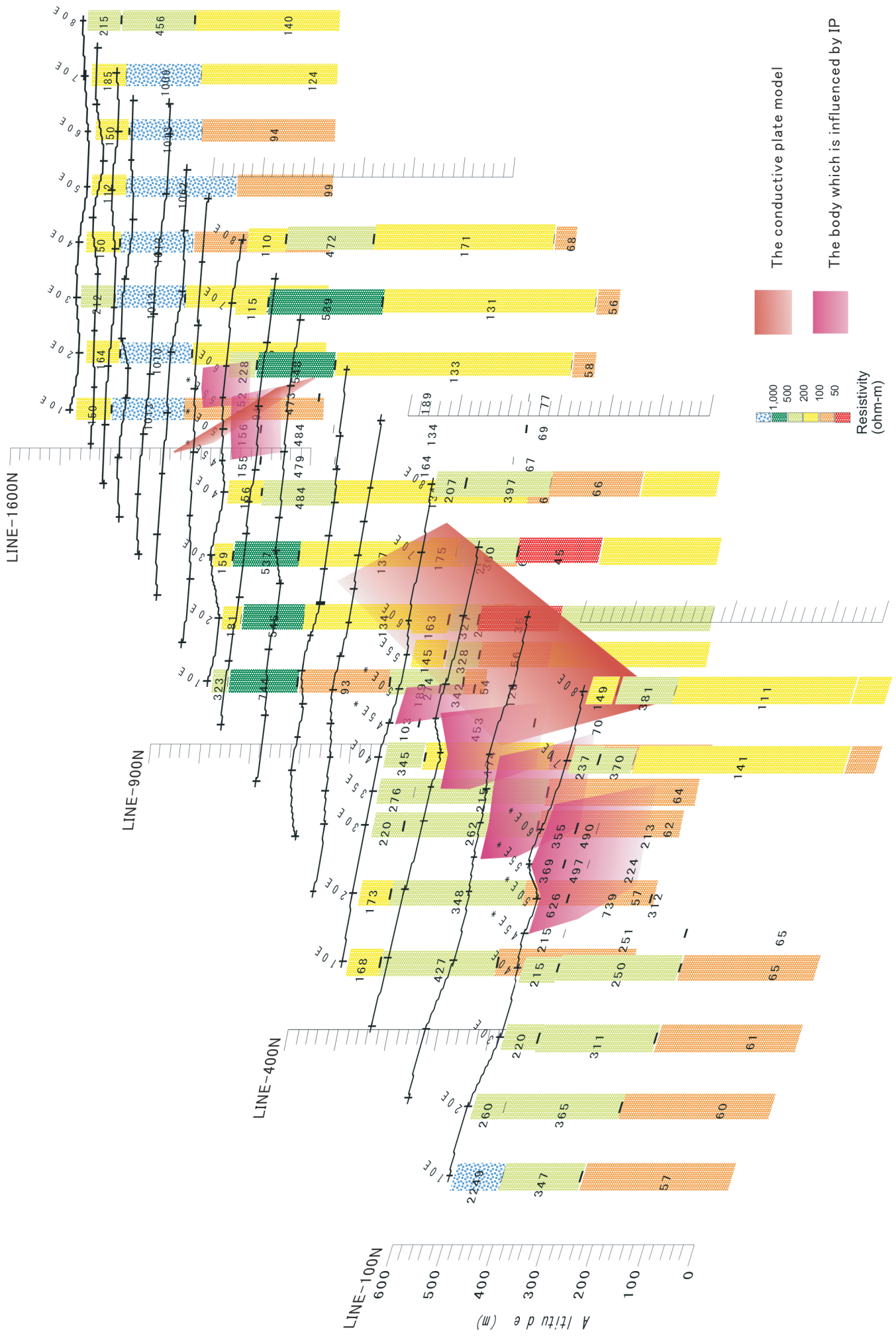


Fig. II-2-2-10 The resistivity structure model by TEM in Azzouz

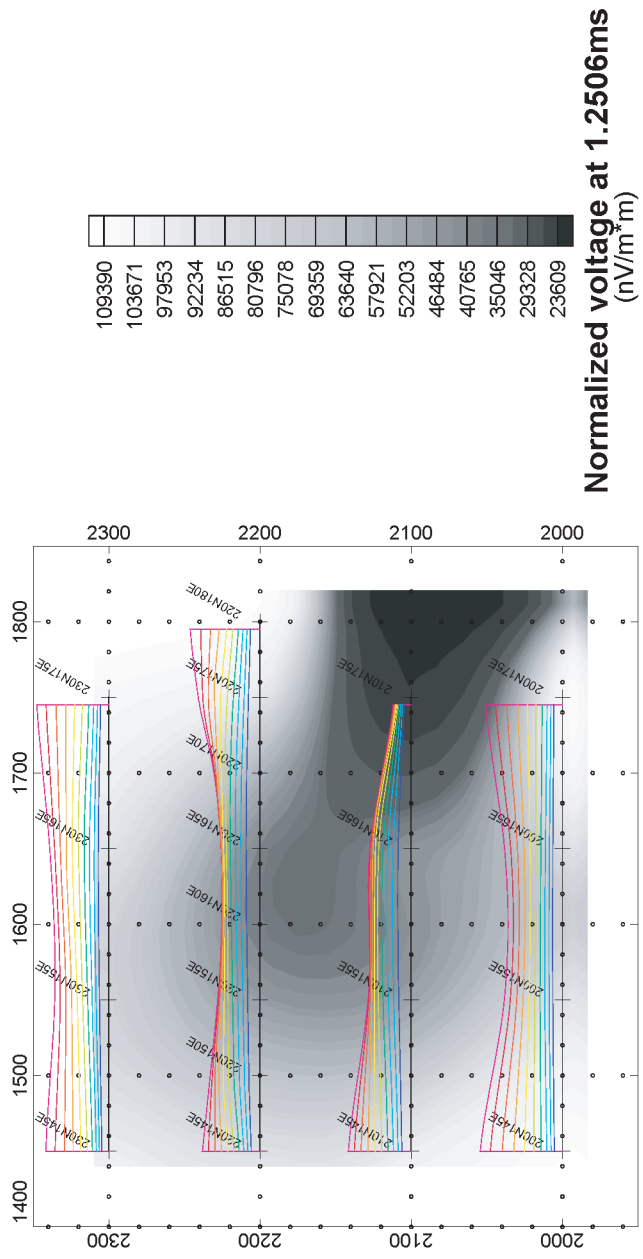


Fig. II-2-2-11 Normalized voltage profiles in Khefawna

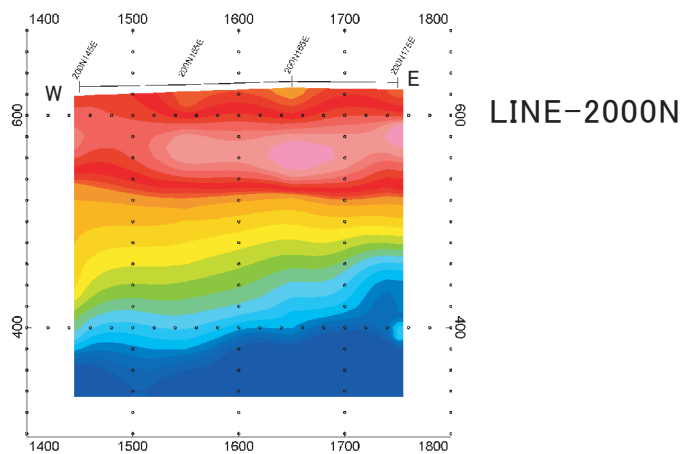
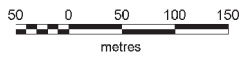
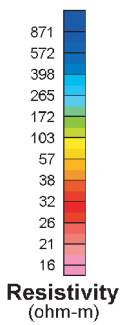
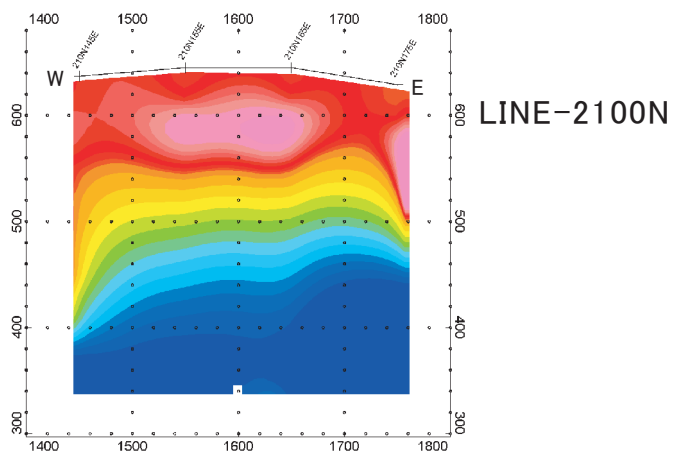
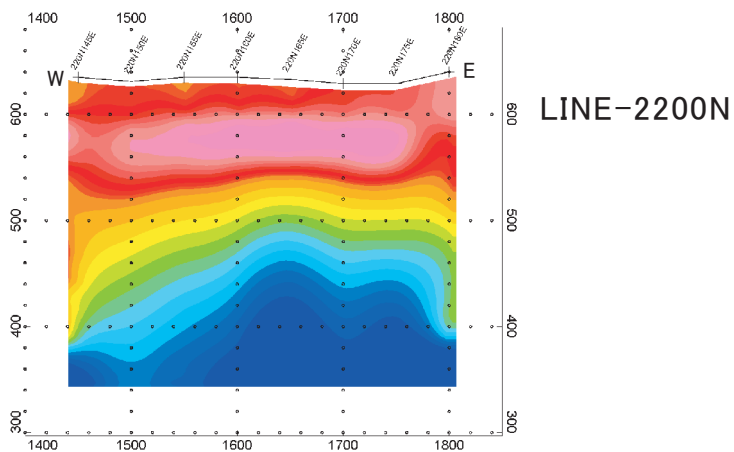
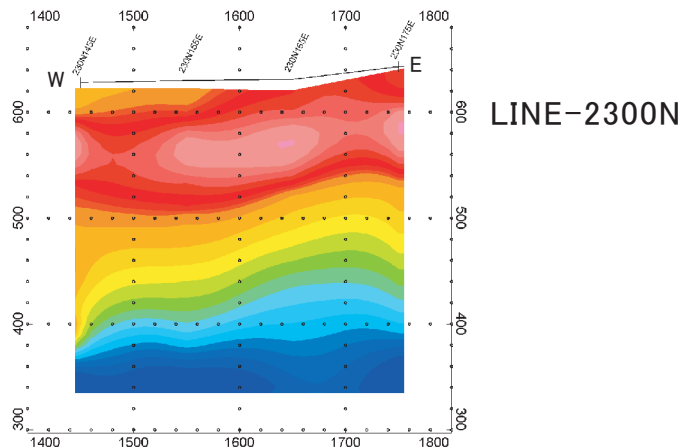


Fig. II-2-2-12 Resistivity structure sections by TEM in Khefawna

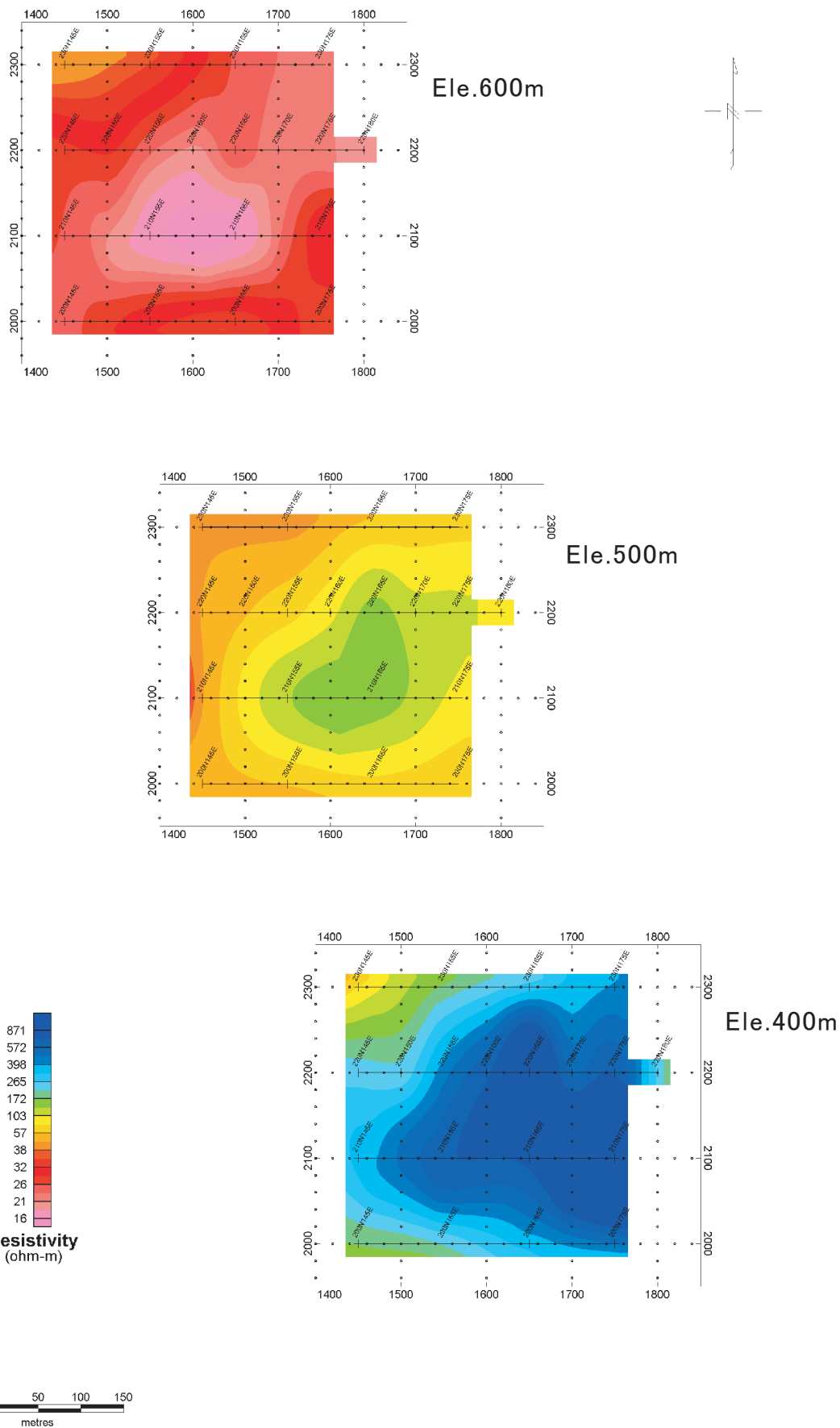


Fig. II-2-2-13 Resistivity distribution maps by TEM in Khefawna

Table II-2-2-2 Parameter of plate model

line	gate	Resistivity of host rock (ohm-m)	Thin Sheet below surface		size		position			strike (deg)	dip (deg)	Plunge (deg)	Conductance (S)	Amplitude of response
			Conductance (S)	Depth (m)	Length (m)	Depth (m)	X (m)	Y (m)	Z (m)					
300N	1-5	600	0.01	50	400	350	575	350	-10	N30° E	70E	0	1.8	2.9
	6-10	600	0.01	50	400	350	555	350	-10	N30° E	70E	0	5.5	1.7
	11-15	600	0.01	50	400	350	555	350	-10	N30° E	70E	0	12.4	1.0
	16-20	600	0.01	50	400	350	555	350	-10	N30° E	70E	0	36.6	0.3
350N	1-5	600	0.01	50	400	350	575	350	-10	N30° E	85E	0	2.0	2.4
	6-10	600	0.01	50	400	350	575	350	-10	N30° E	85E	0	5.6	1.1
	11-15	600	0.01	50	400	350	550	350	-10	N30° E	70E	0	15.6	0.8
	16-20	600	0.01	50	400	350	550	350	-10	N30° E	70E	0	26.1	0.4
400N	1-5	600	0.01	50	400	350	577	350	-10	N30° E	85E	0	1.8	2.4
	6-10	600	0.01	50	400	350	560	350	-10	N30° E	70E	0	0.1	1.2
	11-15	600	0.01	50	400	350	540	350	-10	N30° E	50E	0	15.9	0.6
	16-20	600	0.01	50	400	350	548	350	-10	N30° E	45E	0	31.6	0.2
850N	1-5	240	0.29	50	300	200	518	900	-32	N10° E	70E	0	1.5	9.7
	6-10	300	0.29	50	300	200	518	900	-32	N10° E	70E	0	1.5	7.3
	11-15	240	0.29	50	300	200	518	900	-32	N10° E	70E	0	1.5	7.3
	16-20	180	0.29	50	300	200	518	900	-32	N10° E	70E	0	1.5	7.3
900N	1-5	240	0.29	50	300	200	518	900	-32	N10° E	70E	0	1.5	7.3
	6-10	240	0.29	50	300	200	518	900	-32	N10° E	70E	0	1.5	7.3
	11-15	230	0.29	50	300	200	518	900	-32	N10° E	70E	0	1.5	7.3
	16-20	180	0.29	50	300	200	518	900	-32	N10° E	70E	0	1.5	7.3
950N	1-5	240	0.29	50	300	200	518	900	-32	N10° E	70E	0	1.5	7.3
	6-10	240	0.29	50	300	200	518	900	-32	N10° E	70E	0	1.5	7.3
	11-15	230	0.29	50	300	200	518	900	-32	N10° E	70E	0	1.5	7.3
	16-20	180	0.29	50	300	200	518	900	-32	N10° E	70E	0	1.5	7.3